TEMPERATURE DEPENDENT EFFECTIVE FRICTION COEFFICIENT ESTIMATION IN FRICTION STIR WELDING WITH THE BOBBIN TOOL

by

Miroslav M. MIJAJLOVIĆ[a]*, Sonja M. VIDOJKOVIĆ[b]
and Miloš S. MILOŠEVIĆ[a]

[a] Faculty of Mechanical Engineering, University of Nis, Nis, Serbia
[b] Institute of Chemistry, Technology and Metallurgy,
University of Belgrade, Belgrade, Serbia

The friction coefficient in many friction stir welding researches is generally used as an effective, constant value without concern on the adaptable and changeable nature of the friction during welding sequence. This is understandable because the main problem in analyzing friction in friction stir welding are complex nature of the friction processes, case-dependent and time dependent contact between the bodies, influence of the temperature, sliding velocity, etc. This paper is presenting a complex experimental-numerical-analytical model for estimating the effective friction coefficient on contact of the bobbin tool and welding plates during welding, considering the temperature at the contact as the most influencing parameter on friction. The estimation criterion is the correspondence of the experimental temperature and temperature from the numerical model. The estimation procedure is iterative and parametric – the heat transport parameters and friction coefficient are adapted during the estimation procedure in a realistic manner to achieve relative difference between experimental and model's temperature lower than 3%. The results show that friction coefficient varies from 0.01 to 0.21 for steel-aluminium alloy contact and temperature range from 406 °C to 22 °C.

Key words: *friction stir welding, temperature, friction coefficient*

Introduction

Friction stir welding (FSW) is a solid state welding process that during last two decades became extremely interesting for many researchers. Tendentiously invented for application on the sheets of mild Al alloys, where common arc welding processes show lower efficiency, lower quality levels and higher costs of operation, FSW became a break-thru joining process applicable to materials different than Al, as well [1]. During years, the FSW process is, more or less successfully described considering different scientific and engineering aspects – starting from application on materials different than Al, recognition and optimization of the process parameters, thermal-mechanical-kinetic modelling of the process, quality and weld properties inspection, usability and efficiency of the process [2]. The friction is often marginally considered as a factor of high impact on the welding process. Even more often, the fric-

---

* Corresponding author: mijajlom@masfak.ni.ac.rs

S1322

Mijajlović, M. M., *et al.*: Temperature Dependent Effective Friction Coefficient …
THERMAL SCIENCE, Year 2016, Vol. 20, Suppl. 5, pp. S1321-S1332

tion and the friction based processes in FSW are considered as a pure number that represents friction coefficient – a number between 0 and 2 [3, 4].

Friction coefficient and FSW bobbin tool

The friction coefficient is a ratio of the frictional load and normal load applied to a mutual contact surface of two bodies while exists a tendency that one body will start moving in the direction of active load's action [5]. In FSW the welding tool and workpieces have a complex contact on more than one surface and the movement is dominantly rotation with slow translation along the joint line [4].

In such a case, it is very difficult to decompose the contact condition, frictional and normal loading to the elementary level applicable in the modelling process.

In this research the butt welding of two plates is done with the fixed bobbin tool [6], starting the welding sequence from the technological hole (fig. 1). The technological hole is prepared in the workpieces, at the joint line and the diameter of the hole is the same as the diameter of the probe. The probe is mounted into the technological hole and the bobbin tool is tightened with the bobbin tool's nut, creating the stabile working welding configuration. In
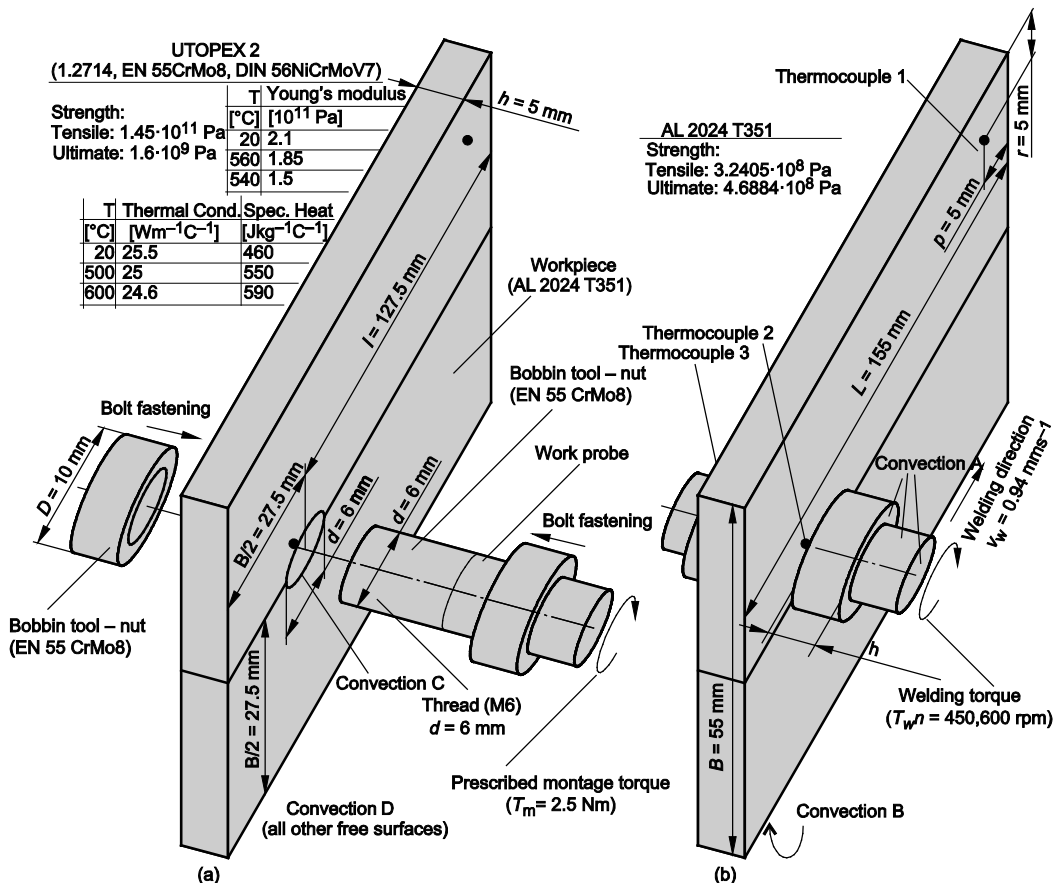

Figure 1. Schematic of the FSW process with bobbin tool; (a) mounting welding tool, (b) mounted welding tool

such a design concept, active surfaces of the tool are shoulder tip at the bolt and nut and the probe. The normal load at the active surfaces is the contact pressure induced by bolt tightening, thermal expansion and working regimes of the welding. The frictional loads at the contact are induced with the welding torque and welding force [4, 5].

Friction coefficient estimation methodology

The friction coefficient estimation methodology used in this research combines analytical, numerical and experimental models that are mutually connected and share the results – it is a mix of experimental results, analytical approach and numerical analysis.

The friction coefficient is estimated in two phases (fig. 2), using *step by step* approach and iterative search for the convergence of the model/solution.

During the first phase of the estimation procedure, the complete system is prepared and mounted as for the welding sequence. The system is heated in the induction furnace to 450 °C and left in the room, at environmental temperature of 22 °C to cool down without intentional thermal disruptions. Temperatures at the thermocouples i (i = 1, 2, and 3) mounted on the system (fig. 1) are measured and recorded during the complete cooling sequence. This part of the estimation is done under experimental model 1 (EM1) (fig. 2).
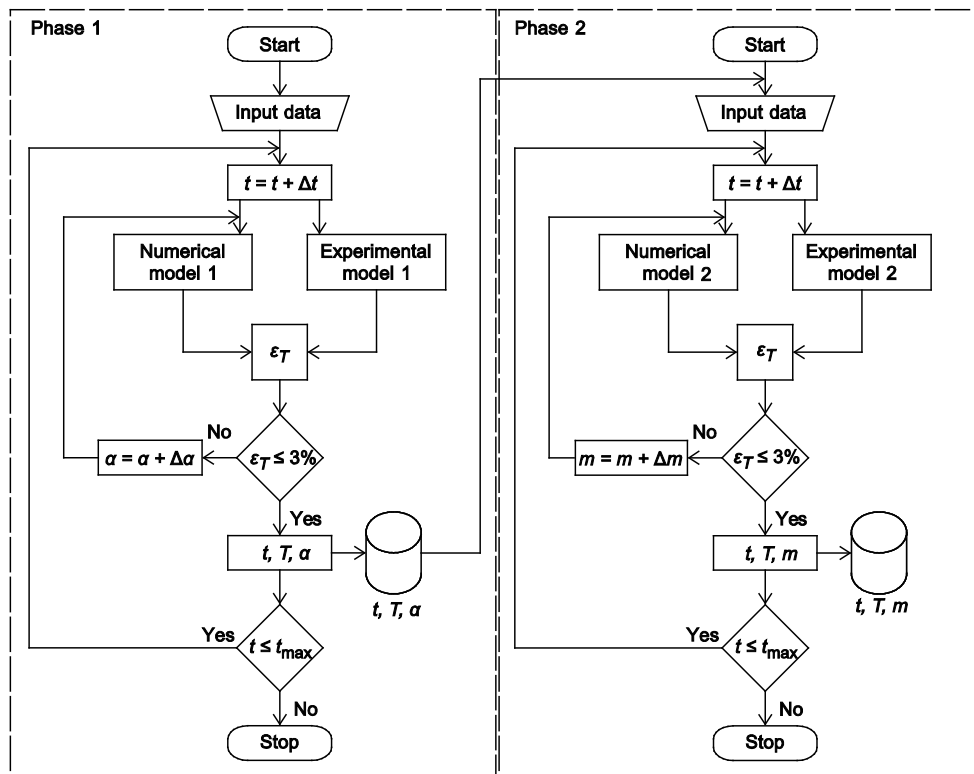

Figure 2. Algorithm of friction coefficient estimation

The system used in EM1 is modelled as a computer-aided design (CAD) model, discretized in the finite element (FE) domain and prepared for the transient-thermal numerical

S1324

Mijajlović, M. M., *et al.*: Temperature Dependent Effective Friction Coefficient …
THERMAL SCIENCE, Year 2016, Vol. 20, Suppl. 5, pp. S1321-S1332

simulation in the ANSYS Workbench. Transient-thermal simulation model in ANSYS is used only to simulate heat transportation thru the system. The simulation is done under numerical model 1 (NM1) (fig. 2). The goal of the simulation is to adapt the heat transportation conditions of the NM1 (conduction and convection coefficients at important parts of the system) in order to reach the real heat transport conditions of EM1. The procedure of conduction and convection heat transport adaptation is iterative and discrete – the nominal heat transportation coefficients are an input into NM1, simulation is run and the numerical temperatures are obtained. Afterwards, the temperatures at the thermocouples from EM1 are compared to the temperatures at the proper FE nodes in NM1. The temperature dependent heat transportation coefficients for each discrete moment of time are adapted until the relative difference of the temperatures from EM1 and NM1 become ≤3% and then the procedure is repeated for the new discretized moment of time. An output of the simulation are by temperature depended convection and conductance coefficients of the system, usable for further simulating FSW process on the system. The duration of the first phase of the friction coefficient estimation lasted approximately 60 hours.

The second phase of estimation starts with the experimental welding of the parts using prescribed welding parameters. The rotation rate of the welding tool is limited to 450 rpm but proper welding can be done with rotation rate up to 600 rpm. This model is named experimental model 2 (EM2). During welding, the monitoring system has been capturing temperatures at the thermocouples, torque and the force reactions of the support (point B, fig. 2). Also, the model EM2 is CAD modelled, FE discretized and prepared for the transient-structural fully coupled simulation in ANSYS Workbench. The model uses SOLID226 hex 1st order 3-D elements and CONTA/TARGET contact elements capable to capture frictional heating and plastic deformation of bodies on contact. This model is named numerical model 2 (NM2). The heat transfer coefficients from the NM1 are embedded into the NM2. Since NM2 requires significant computer resources and computational time, the simulations of EM2 is done only until the quasi continuous temperature trend or maximal temperature from the EM2 is reached. Similarly to the criterion in the first phase, relative difference of temperatures from EM2 and NM2 is the criterion of convergence for the coefficient of friction. The temperature dependent friction coefficients for the discrete moment of time and contact between bodies are adapted until the relative difference of the temperatures from EM2 and NM2 become ≤3% and then the procedure is repeated for the new discretized moment of time. The output from the simulation is the temperature dependent coefficient of friction in FSW.

The initial friction coefficient for the EM2 simulation is taken as a calculated effective value from the adapted analytical-numerical method for estimation of the friction coefficient. The reason for such an approach was to improve the starting convergence of the simulation using realistic values of the friction coefficient.

Adapted analytical-numerical method for estimation of the friction coefficient

The basic assumption of the model for estimating the friction coefficient is that the most of the invested mechanical energy (the welding torque) is transformed into frictional and deformational heat [7-9]. The model is functional in the second phase of the estimation – the heat transportation coefficients from the first phase are used as input data of the model. Furthermore, the welding sequence is simulated both in realistic experiment and numerically, where data obtained in the realistic experiment are used as reference data for numerically obtained data.

The system of the bobbin tool mounted on the workpiece is supported by the clamping system of the working machine (point A, fig. 1) but enables rotation of the system along z-axis and translation of the welding tool along x-axis. The second support point of the system is the lover edge of the workpiece (point B, fig. 2) which restrains translations of the workpiece in all directions. The torque T_w and welding force F delivered to the welding tool induce reaction forces X_B and Y_B in the support B. The horizontal component of the reaction is adequate to the welding force (eq. 1) and the vertical component is equal to the weight of the system (eq. 2). The loads from the welding tool and reaction forces are function of time (*t*) [10].

The welding torque T_w delivered to the welding tool consists of two components – frictional component of the torque T_{fr} and the rest of the torque T_{res}. The frictional component of the torque is in equilibrium with the frictional resistance of the contact pair welding tool-workpiece. The rest of the applied torque is used during the welding process.

$$\sum_{i=1}^{n} X_i(t) = 0, \qquad X_B(t) \geq F(t) \quad (1)$$

$$\sum_{i=1}^{n} Y_i(t) = 0, \qquad Y_B(t) \geq G \quad (2)$$

$$\sum_{i=1}^{n} M_A(t) = 0$$

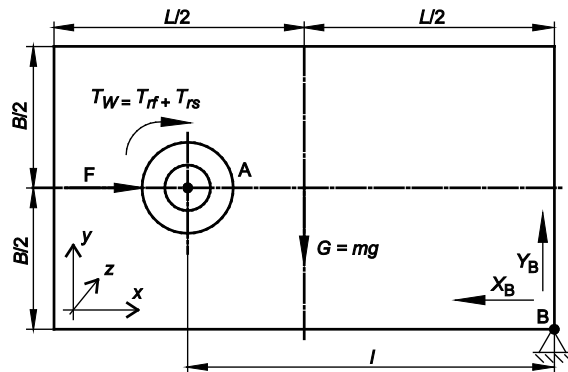$$T_{fr}(t) = \frac{2lY_B(t) - G(2l - L) - X_B(t)B}{2} \quad (3)$$

Figure 3. Scheme of the equilibrium conditions

Assuming that only the frictional component of the torque is inducing the reactions in the support B (fig. 3), the equation of momentum's equilibrium gives the amount of frictional component of the torque (eq. 3).

Active surfaces of the welding tool (fig. 4) are probe (p), shoulder tip on the nut (sn) and shoulder tip on the bolt (sb) induce frictional reactions to the frictional component of the torque – momentum of friction (eq. 4):

$$T_{fr}(t) = T_{fr\text{-}p}(t) + T_{fr\text{-}sn}(t) + T_{fr\text{-}sb}(t) \quad (4)$$

where $T_{fr\text{-}p}(t)$ is the momentum of friction of the probe, $T_{fr\text{-}sn}(t)$ – the momentum of friction on the shoulder tip of the nut, and $T_{fr\text{-}sb}(t)$ – the momentum of friction on the shoulder tip of the bolt.

Figure 4. Welding tool's active surfaces

The momentum of friction on the shoulder tip of the nut is:

$$T_{fr\text{-}sn}(t) = 2\pi \int_{0.5d}^{0.5D} r^2 \mu_{sn}(r,t) p_{sn}(r,t) \, dr \qquad (5)$$
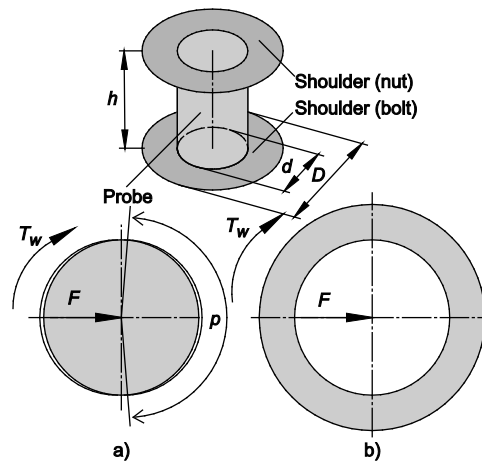
S1326

Mijajlović, M. M., *et al.*: Temperature Dependent Effective Friction Coefficient ...
THERMAL SCIENCE, Year 2016, Vol. 20, Suppl. 5, pp. S1321-S1332

where d [mm] is the diameter of the probe and inner diameter of the nut/bolt, D [mm] – the outer diameter of the shoulder, $\mu_{sn}(r, t)$ [–] – the friction coefficient distribution on the shoulder tip of the nut, and $p_{sn}(r, t)$ [MPa] – the contact pressure distribution on the shoulder tip of the nut.

Assuming that friction coefficient distribution and contact pressure distribution are uniform (median):

$$\mu_{msn}(t) = \mu_{sn}(r,t), \qquad p_{msn}(t) = p_{sn}(r,t) \tag{6}$$

where $\mu_{msn}(r, t)$ [–] is the median friction coefficient on shoulder tip of the nut, $p_{msn}(t)$ [MPa] – the median contact coefficient on shoulder tip of the nut [MPa]. The momentum of friction on the shoulder tip of the nut becomes:

$$T_{fr\text{-}sn}(t) \approx 2\pi p_{msn}(t)\mu_{msn}(t) \int\limits_{0.5d}^{0.5D} r^2 \mathrm{d}r = \frac{\pi}{12} p_{msn}(t)\mu_{msn}(t)(D^3 - d^3) \tag{7}$$

Using the same principle, the momentum of friction on the shoulder tip of the bolt becomes:

$$T_{fr\text{-}sn}(t) \approx \frac{\pi}{12} p_{msb}(t)\mu_{msb}(t)(D^3 - d^3) \tag{8}$$

where $\mu_{msb}(r, t)$ [–] is the median friction coefficient on shoulder tip of the bolt, $p_{msb}(t)$ [MPa] – the median contact pressure on shoulder tip of the bolt.

The momentum of friction on the probe, using median contact pressure and friction coefficient on the probe, is:

$$T_{fr\text{-}p}(t) = \frac{d}{2} F_{\mu p}(t) = \frac{d}{2}\mu_{mp}(t) p_{mp}(t) \frac{\theta_p}{2\pi} d\pi h \tag{9}$$

where $F_{\mu p}(t)$ [N] is the friction force on the probe, $\mu_{mp}(t)$ [–] – the median friction coefficient on the probe, $p_{mp}(t)$ [MPa] – the median contact pressure on the probe, θ_p [rad] – the effective contact angle of the probe *vs.* workpiece, and h [mm] – the height of the probe.

Assuming that effective contact angle $\theta_p = \pi$ rad, fig. 2(a), the momentum of friction on the probe becomes:

$$T_{fr\text{-}p}(t) = \frac{\pi}{4}\mu_{mp}(t) p_{mp}(t) d^2 h \tag{10}$$

Summarizing the partial momentums of friction, total momentum of friction is:

$$T_{fr}(t) = \frac{\pi}{4} d^2 h \mu_{mp}(t) p_{mp}(t) + \frac{\pi}{12}(D^3 - d^3)[p_{msn}(t)\mu_{msn}(t) + p_{msb}(t)\mu_{msb}(t)] \tag{11}$$

Since the main goal of the modeling is estimation of the effective friction coefficient on welding tool, partial median friction coefficients on active surfaces are assumed equal:

$$\mu_e(t) = \mu_{mp}(t) = \mu_{msn}(t) = \mu_{msb}(t) \tag{12}$$

and after transformation, eq. (12) gives the effective friction coefficient on the welding tool:

$$\mu_e(t) = \frac{12 T_{fr}(t)}{\pi \{3d^2 h p_{mp}(t) + (D^3 - d^3)[p_{msn}(t) + p_{msb}(t)]\}}$$ (13)

The effective friction coefficient (eq. 13) is used only as an initial input value for the numerical FEM model in the first calculation step – the usable and requested result is by temperature dependent friction coefficient $\mu_e(T)$. Afterwards numerical model uses median friction coefficients for every active surface, respectively. The model is estimating the amount of heat generated on active surfaces and temperature of every discrete node of the model and after reaching convergence of the results, the model stops further calculation and performs comparison of the temperatures in tendentiously selected points from the experimental (T_e) and numerical (T_n) models, in discrete points $i = 1, 2, 3$:

$$\varepsilon_T(t)_i = \frac{\left| T_e(t)_i - T_n(t)_i \right|}{\left| T_e(t)_i \right|} 100\%, \qquad i = 1, 2, 3$$ (14)

The criterion of the relative difference of temperatures $\varepsilon_T(t)_i$ is set to 3%:

$$\varepsilon_T(t)_i \begin{cases} \leq 3\%, & \begin{cases} \mu_{mp}(t + \Delta t) = \mu_{mp}(t) \\ \mu_{msn}(t + \Delta t) = \mu_{msn}(t) \\ \mu_{msb}(t + \Delta t) = \mu_{msb}(t) \end{cases} \\ > 3\%, & \begin{cases} \mu_{mp}(t) = \mu_{mp}(t) \pm \mu_{mp}(t,T) \\ \mu_{msn}(t) = \mu_{msn}(t) \pm \mu_{msn}(t,T) \\ \mu_{msb}(t) = \mu_{msb}(t) \pm \mu_{msb}(t,T) \end{cases} \end{cases}, \qquad i = 1, 2, 3$$ (15)

If the relative difference of temperatures has values for all *i*-s equal and/or smaller than 3%, it is considered that the friction coefficient has an adequate value and as such is used for calculations in the next time moment ($t + \Delta t$). If the relative difference is greater than 3%, the model adapts median friction coefficients for every active surface and repeats the complete calculation step until the convergence is reached. After this, the model is checking the criterion of the relative temperature difference, and continues the procedure. Depending on the results, the model goes to the next time step or goes back to median friction coefficient adaptation.

Results

The temperature of the system in EM1 has been estimated at 3 discrete places by thermocouples. The temperature of the discretized CAD model (fig. 5) is obtained numerically in all discrete nodes using ANSYS. The temperature is estimated using adapted convection parameters at surfaces A, B, C, and D, following the convergence and given temperature criterion. For comparison with the experimental results, the temperature from NM1 at the node 3320, that is located at the position of the thermocouple 1, is given in fig. 6.
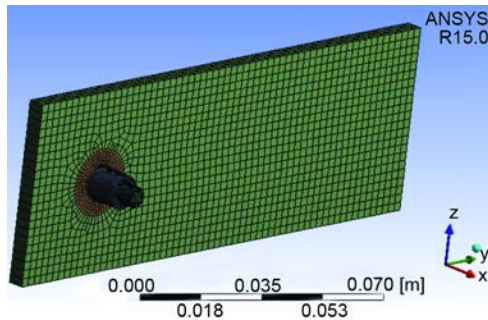
S1328

Mijajlović, M. M., *et al.*: Temperature Dependent Effective Friction Coefficient …
THERMAL SCIENCE, Year 2016, Vol. 20, Suppl. 5, pp. S1321-S1332

Figure 5. The FEA model of the structure in ANSYS Workbench R15.0
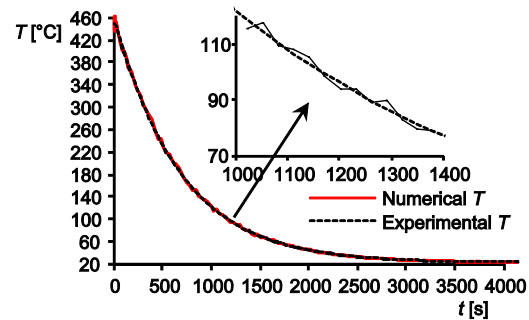

Figure 6. Experimental temperature from EM1@thermocouple 1 and numerical temperature from NM1@Node 3320

The adaptation of convection heat loses at surfaces A, B, C, and D is done iteratively and simultaneously for all the surfaces during the welding sequence, respecting the temperature criterion. Afterwards, the median temperatures of all surfaces are estimated and heat convection factors *vs.* temperatures are presented.

Figures 7 and 8 show the heat convection parameters *vs.* time and heat convection parameters *vs.* median temperature of the convective surfaces A, B, C, and D, respectively. The thick line is representing the values where heat convection factors enable fulfillment of the temperature criterion, while dotted values are iteration attempts. The functional relationship of the heat convection factor and time/temperature are given in figs. 7 and 8, as well.
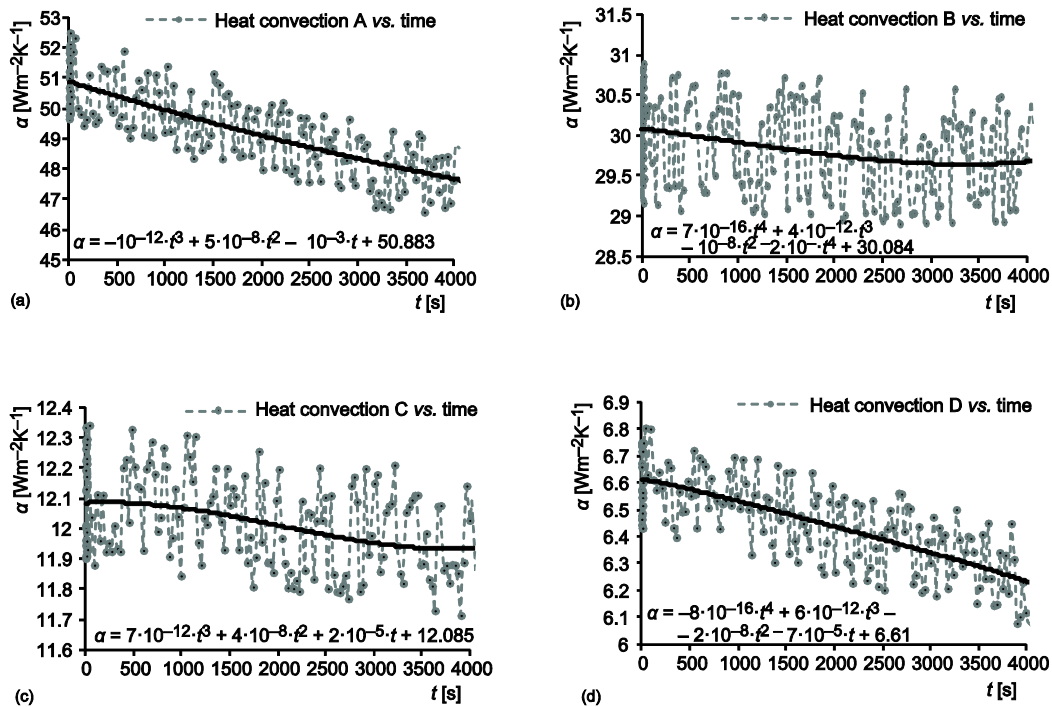

(a)

$\alpha = -10^{-12} \cdot t^3 + 5 \cdot 10^{-8} \cdot t^2 - 10^{-3} \cdot t + 50.883$

(b)

$\alpha = 7 \cdot 10^{-16} \cdot t^4 + 4 \cdot 10^{-12} \cdot t^3 - 10^{-8} \cdot t^2 - 2 \cdot 10^{-4} \cdot t + 30.084$

(c)

$\alpha = 7 \cdot 10^{-12} \cdot t^3 + 4 \cdot 10^{-8} \cdot t^2 + 2 \cdot 10^{-5} \cdot t + 12.085$

(d)

$\alpha = -8 \cdot 10^{-16} \cdot t^4 + 6 \cdot 10^{-12} \cdot t^3 - 2 \cdot 10^{-8} \cdot t^2 - 7 \cdot 10^{-5} \cdot t + 6.61$

Figure 7. Heat convection factor at convective surfaces *vs.* time

Mijajlović, M. M., *et al.*: Temperature Dependent Effective Friction Coefficient …
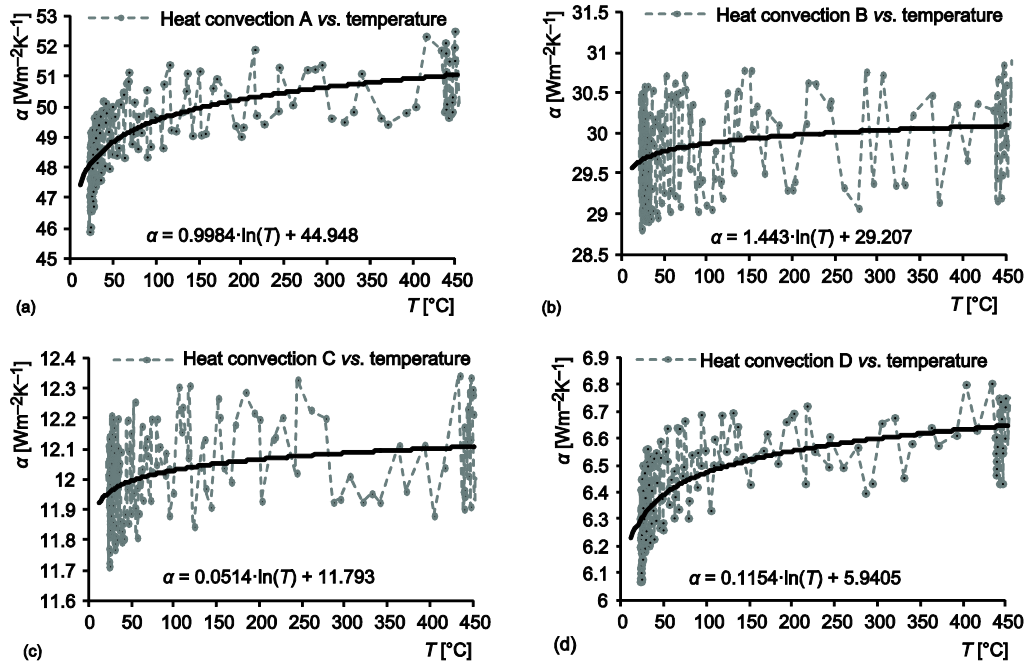THERMAL SCIENCE, Year 2016, Vol. 20, Suppl. 5, pp. S1321-S1332

S1329

Figure 8. Heat convection factor at convective surfaces *vs.* median temperature of the surface

To estimate the friction coefficient on active surfaces of the welding tool, it is necessary to fulfill the temperature criteria of acceptance. Following the criteria, the effective friction coefficient is involved in the NM2 as an adaptation coefficient for reaching temperatures from the EM2.

Using iterative approach with a large number of repetitions, the friction coefficient (fig. 9) has been adapted to reach numerical temperatures of the welding tool's active surfaces (fig. 10) within the tolerance of 3%. Having both the average temperatures and average friction coefficient at active surfaces the relationship between the effective friction coefficient and average temperature at the active surfaces is made (fig. 11).
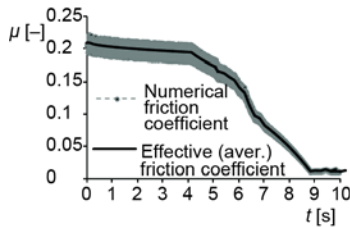

Figure 9. Numerical and effective (average) friction coefficient *vs.* time at the active surfaces of the welding tool
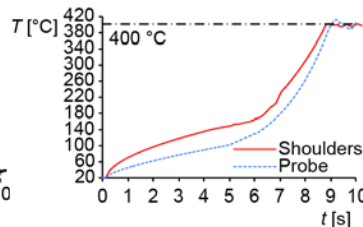
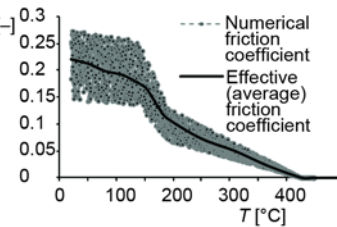**Figure 10. Numerically estimated average temperatures at the shoulders and probe of the bobbin tool**

Figure 11. Effective (average) friction coefficient *vs.* median temperature at the active surfaces of the welding tool

S1330

Mijajlović, M. M., *et al.*: Temperature Dependent Effective Friction Coefficient …
THERMAL SCIENCE, Year 2016, Vol. 20, Suppl. 5, pp. S1321-S1332

Discussion and conclusions

The friction processes and friction coefficient in friction stir welding are only marginally investigated regardless on twenty five years of FSW's existence. The intentional simplification of the situation is: friction in the FSW is complex and extremely case-dependent parameter. Presently, there are no known frictional models that might unilaterally recognize what and how does this affect the friction coefficient.

It is very difficult to recognize and analyze influence of all parameters on friction regardless on used model. Therefore, the model presented in this research is based on three assumptions:
(1) the main factor affecting friction coefficient is temperature at the contact surfaces (other parameters like strain, sliding velocity, roughness, *etc.* are neglected),
(2) the effective friction coefficient is considered to be the same on all active surfaces, and
(3) the temperature change of materials is majorly inflicted by frictional heat what makes a direct relationship between friction coefficient and temperature.

The presented model is combining experimental, analytical and numerical analysis and the results from each, uses complex coupled structural-transient mechanical analysis in ANSYS Workbench in a numerical iterative mode. This approach is computer time demanding but always gives converging results.

The friction coefficient on contact between bobbin tool and AL welding plates at environmental temperature of 22 °C has a value of 0.21 and decreases with temperature increase. The temperature reaches maximum of 406 °C and the friction coefficient reaches a minimum of 0.01. The friction coefficient and temperature always have nonlinear and inverse relationship – the increase of temperature decreases friction coefficient and vice versa.

Acknowledgment

Data sheet

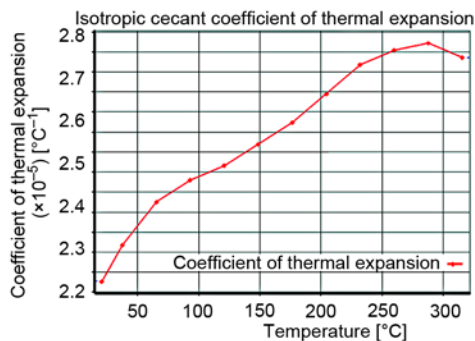Figures 12-15 give properties of AL 2024 T351.

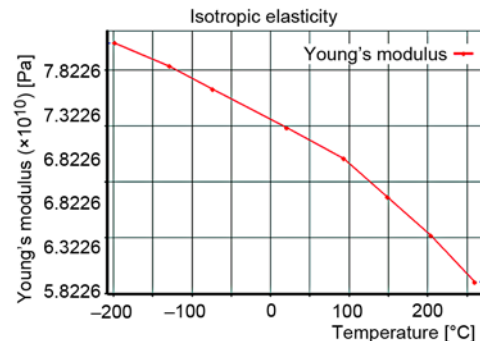**Figure 12. Thermal expansion coefficient**
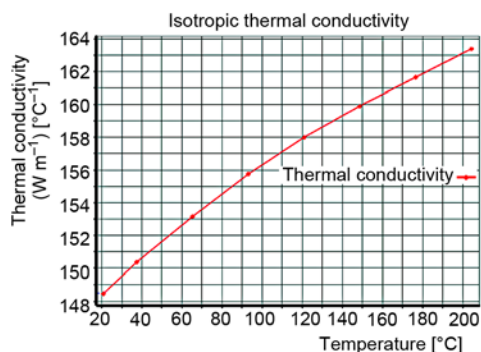

Figure. 13 Isotropic elasticity
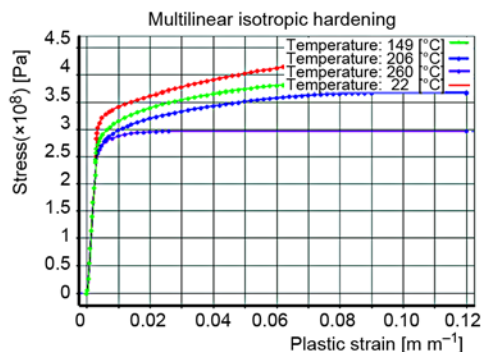
Figure 14. Thermal conductivity

Figure 15. Isotropic hardening

Nomenclature

B – width of the welding plates, [m]
D – diameter of the shoulder, [m]
d – diameter of the probe, [m]
G – weight of welding plates, [N]
h – height of the welding plate/shoulder, [m]
L – length of the welding plate, [m]
L_{wt} – length of the welding tool, [m]
l – welding length, [m]
$M_A(t)$ – reaction momentum in A dependent on time t, [Nm]
m – mass of welding plates, [kg]
n – revolutions per minute, [min^{-1}]
p – distance of the thermocouple 1 from the closer vertical edge on welding plate, [m]
r – distance of the thermocouple 1 from the closer horizontal edge on welding plate, [m]
T – temperature, [°C]
T_{fr} – frictional component of torque, [Nm]
T_n – prescribed montage torque, [Nm]
T_{res} – rest of torque, [Nm]

T_w – welding torque, [Nm]
t – time, [s]
Δt – time interval, [s]
$X_A(t)$ – reaction force in A, in x-direction dependent on time t, [N]
$X_B(t)$ – reaction force in B, in x-direction dependent on time t, [N]
$X_i(t)$ – force component in x-direction dependent on time t, [N]
$Y_A(t)$ – reaction force in A, in y-direction dependent on time t, [N]
$Y_B(t)$ – reaction force in B, in y-direction dependent on time t, [N]
$Y_i(t)$ – force component in y-direction dependent on time t, [N]
$Z_i(t)$ – force component in z-direction dependent on time t, [N]

Greek symbols

α – surface convection parameter, [Wm^{-1}°C^{-1}]
ε_T – relative temperature difference, [%]
μ – friction coefficient, [–]

References

[1] Soundararajan, V., *et al.*, An Overview of R&D Work in Friction Stir Welding at SMU, MJoM, Metalurgija, Association of Metallurgical Engineers of Serbia, *Journal of Metallurgy, 204* (2006), 12, pp. 277-295
[2] Kalle, S., Application of Friction Stir Welding in the Shipbuilding Industry, *Proceedings,* Lightweight Construction – Latest Development, London, 2000
[3] Kumar, K., *et al.,* An Investigation of Friction during Friction Stir Welding of Metallic Materials, *Materials and Manufacturing Processes, 24* (2009), 4, pp. 438-44
[4] Mijajlović, M., Investigation and Development of Analytical Model for Estimation of Amount of Heat Generated During FSW, Ph. D., University of Nis, Nis, Serbia, 2012
[5] Miltenović, A., *et al.,* Determination of Friction Heat Generation in Wheel-Rail Contact Using FEM, *Facta Universitatis: Mechanical Engineering, 13* (2015), 2, pp. 99-108
[6] Zettler, R., *et al.*, A Study of Material Flow in FSW of AA2024-T351 and AA 6056-T4 Alloys, *Proceedings,* the 5th International Conference on Friction Stir Welding, Metz, France, 2004

S1332

Nakoryakov, V. E., *et al.*: Helium Production Technology Based on Natural Gas …
THERMAL SCIENCE, Year 2016, Vol. 20, Suppl. 4, pp. S1321-S1332

[7] Schmidt, H., *et al.,* An Analytical Model for the Heat Generation in Friction Stir Welding, *Modelling and Simulation in Materials Science and Engineering, 12* (2004), 1, pp. 143-157

[8] Veljić, D., *et al.,* Heat Generation during Plunge Stage in Friction Stir Welding, *Thermal Science, 17* (2013), 2, pp. 489-496

[9] Heurtier, P., *et al.,* Mechanical and Thermal Modelling of Friction Stir Welding, *Journal of Materials Processing Technology, 171* (2006), pp. 348-357

[10] Mijajlović, M. *et al.,* Study About Friction Coefficient Estimation in Friction Stir Welding, Balkantrib 11, *Proceedings,* 7th International Conference on Tribology, Thessaloniki, Greece, 2011, pp. 323-330